Biophysical Journal Volume 71 September 1996 1450–1461

Effects of MgATP and MgADP on the Cross-Bridge Kinetics of Rabbit Soleus Slow-Twitch Muscle Fibers

Gang Wang and Masataka Kawai
Department of Anatomy, The University of Iowa, Iowa City, Iowa 52242 USA

ABSTRACT The elementary steps surrounding the nucleotide binding step in the cross-bridge cycle were investigated with sinusoidal analysis in rabbit soleus slow-twitch muscle fibers. The single-fiber preparations were activated at pCa 4.40, ionic strength 180 mM, 20°C, and the effects of MgATP (S) and MgADP (D) concentrations on three exponential processes B, C, and D were studied. Our results demonstrate that all apparent (measured) rate constants increased and saturated hyperbolically as the MgATP concentration was increased. These results are consistent with the following cross-bridge scheme:

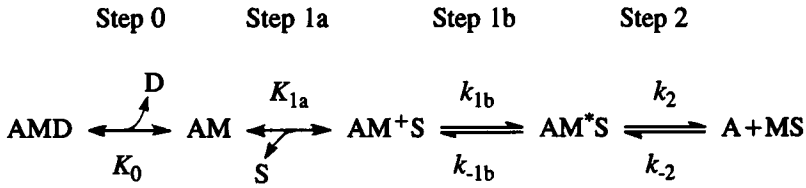

where A = actin, M = myosin, S = MgATP, and D = MgADP. AM^+S is a collision complex, and AM*S is its isomerized form. From our studies, we obtained $K_0 = 18 \pm 4$ mM^{-1} (MgADP association constant, $N = 7$, average ± sem), $K_{1a} = 1.2 \pm 0.3$ mM^{-1} (MgATP association constant, $N = 8$ hereafter), $k_{1b} = 90 \pm 20$ s^{-1} (rate constant of ATP isomerization), $k_{-1b} = 100 \pm 9$ s^{-1} (rate constant of reverse isomerization), $K_{1b} = 1.0 \pm 0.2$ (equilibrium constant of isomerization), $k_2 = 21 \pm 3$ s^{-1} (rate constant of cross-bridge detachment), $k_{-2} = 14.1 \pm 1.0$ s^{-1} (rate constant of reversal of detachment), and $K_2 = 1.6 \pm 0.3$ (equilibrium constant of detachment). K_0 is 8 times and K_{1a} is 2.2 times those in rabbit psoas, indicating that nucleotides bind to cross-bridges more tightly in soleus slow-twitch muscle fibers than in psoas fast-twitch muscle fibers. These results indicate that cross-bridges of slow-twitch fibers are more resistant to ATP depletion than those of fast-twitch fibers. The rate constants of ATP isomerization and cross-bridge detachment steps are, in general, one-tenth to one-thirtieth of those in psoas.

INTRODUCTION

The main function of muscle is to generate force and convert the energy of ATP hydrolysis into useful work. Therefore, it is advantageous to use a system that retains the ability of generating force such as muscle fibers to study the mechanism of force generation. However, there are complications in using the intact muscle fiber system. These include the sarcoplasmic reticulum, which is involved in Ca^{2+} cycling, and the complex system of metabolism that generates ATP in part and removes ADP and phosphate. In contrast, with skinned fibers the function of the sarcoplasmic reticulum is destroyed and the intracellular milieu can be controlled while keeping the contractile apparatus intact. With these preparations, one can apply mechanical and chemical perturbations at the same time, so that more hypotheses can be tested. Unlike solution studies of isolated contractile proteins (White and Taylor, 1976; Marston and Taylor, 1980), in skinned fiber experiments ionic strength can be elevated to that of the physiological level, thereby producing results that should reflect more realistic mechanisms of energy transduction. Thus, skinned fibers provide a simplified model for the study of the mechanism of force generation.

By using the sinusoidal analysis technique on skinned rabbit psoas fibers and ferret myocardium, we studied the effects of MgATP, MgADP, and phosphate (P_i) on the cross-bridge kinetics of rabbit psoas and ferret cardiac fibers (Kawai and Halvorson, 1989, 1991; Zhao and Kawai, 1993; Kawai et al., 1993). Based on these studies, we deduced a cross-bridge scheme consisting of six or seven states (Kawai et al., 1993; Zhao and Kawai, 1993, 1994). We further deduced the association constants of the binding of MgATP and MgADP to cross-bridges, the rate constants of ATP isomerization and cross-bridge detachment steps, and the rate constant of the force generation step. Our success depended largely on the simplification of the cross-bridge scheme by using a principle developed by Hammes (1968), so that an algebraic realization rather than a numeric realization of the apparent rate constants is possible. This sim-

Received for publication 20 December 1995 and in final form 4 June 1996.

Address reprint requests to Dr. Masataka Kawai, Department of Anatomy, University of Iowa, Bowen Science Building, 1–670, Iowa City, IA 52242. Tel.: 319-335-8101; Fax: 319-335-7198; E-mail: mkawai@blue.weeg.uiowa.edu.

0006-3495/96/09/1450/12 $2.00

plification in turn provides an insight into the molecular mechanisms of contraction, which enables further hypotheses to be tested.

Comparison of the kinetic constants among different muscle fiber types is useful in understanding the structure-function relationship and the energy efficiency of slow-twitch fibers (STFs) (Crow and Kushmerick, 1982; Kushmerick et al., 1992a). The comparison may also provide insight into the fundamental mechanism of force generation. The study of STFs is important because of their shared properties with fast-twitch fibers (FTFs) and myocardium: whereas STFs share common structural features with FTFs, STFs share common contractile isoenzymes with myocardium. The study of STFs is also essential to the elucidation of the mechanisms of muscular dystrophy and other muscle diseases, because the majority of human muscles consist of STFs.

We studied the effects of MgATP and MgADP in rabbit soleus STFs and found that these nucleotides bind to cross-bridges more tightly in STFs than in FTFs. We further found that the rate constants of the ATP isomerization and cross-bridge detachment steps of STFs are generally one-tenth to one-thirtieth of those of FTFs. Preliminary accounts of the present results were presented in recent Biophysical Society meetings (Wang et al., 1994; Wang and Kawai, 1995).

MATERIALS AND METHODS

Muscle preparations

New Zealand white rabbits, each weighing 3.5–5 kg, were sacrificed by injecting sodium pentobarbital (150 mg/kg) into an ear vein. The skin of the lower limbs was cut open, and the soleus muscle was exposed, excised, and immersed in the skinning solution (Sk, Table 1) at 0–2°C. Under a dissecting microscope, fiber bundles (about 15 mm in length and 2 mm in diameter) were separated, and at resting length tied to bamboo sticks with silk thread. The bundles were continuously skinned in the Sk solution (Table 1) at 0–2°C for 24 h, and then transferred to a storage solution (mM: 5 EGTA, 2 MgATP, 5 free ATP, 132 potassium propionate, 6000 glycerol, 10 3-(*N*-morpholino)propanesulfonic acid, pH 7.0) and kept at −20°C without freezing.

A single fiber about 10 mm in length was dissected from a stock bundle and transferred to the experimental chamber. Both ends of the preparation were doubly knotted, and one end was connected to the length driver and the other end to the tension transducer. The sarcomere length was adjusted to 2.5 μm as measured by optical diffraction using a He-Ne laser (wavelength 632.8 nm), and then the fiber length (L_0) was determined under the light microscope. Using a medium-power (200×) Normarski optics (Leitz, Diavert), the fiber was carefully monitored, and a damaged fiber was discarded. The diameter was measured by an ocular micrometer, and the cross-sectional area was estimated by assuming a circular cross section.

Standard experimental solutions

Table 1 summarizes the compositions of the solutions used in the experiments. In wash and activating solutions, the ionic strength was maintained at 180 mM with the addition/deletion of potassium and sodium propionates (KProp/NaProp), and the pH was adjusted to 7.00 ± 0.01. An ionic strength of 180 mM was chosen because this is close to the estimated ionic strength in living muscle fibers (Godt and Maughan, 1988). NaN_3 (10 mM) was included to inhibit mitochondrial ATPase. Activating solutions used in the MgATP study included 80 units/ml creatine kinase (CK). In activating solutions of the MgADP study, 0.2 mM P^1,P^5-di(adenosine-5′)pentaphosphate (A_2P_5) was included to inhibit the adelynate kinase, and CP/CK was deleted. Other activating solutions for a specific experiment were made as variations of the control solution. The WS and WD solutions were used to remove EGTA before Ca^{2+} activation in the MgATP study and in the MgADP study, respectively. The WS solution does not have MgATP, Ca^{2+}, or EGTA, but it is otherwise identical to 0S or 5S solutions. Similarly, the WD solution does not have MgADP, Ca^{2+}, or EGTA, but it is otherwise identical to 0D or 3D solutions. Rigor was induced by three washes with Rg_2 solution, followed by the addition of 40 mM EDTA (1:10 by volume), resulting in the Rg_1 solution. The pCa (= $-\log[Ca^{2+}]$) of all activating solutions was 4.40, and free Mg^{2+} was 0.5 mM. The temperature was controlled to 20.0 ± 0.2°C, and the solution in which the muscle fiber was bathed was continuously stirred to minimize local heterogeneities in concentration and temperature.

Experimental procedure

Our earlier work described in detail the method of obtaining the complex modulus data and extracting the apparent rate constants of exponential

TABLE 1 Compositions of the solutions

Solutions	EDTA (mM)	EGTA (mM)	CaEG (mM)	$CaPr_2$ (mM)	MgATP (mM)	ATP (mM)	$MgPr_2$ (mM)	CP (mM)	ADP (mM)	KPi (mM)	KPr (mM)	NaPr (mM)	NaN_3 (mM)	A_2P_5 (mM)	CK (unit/mL)
Sk, Skinning	—	5	—	—	2	5	—	—	—	—	—	132	—	—	—
R, Relaxing	—	5.03	0.97	—	2	5	—	—	—	8	55	61	—	—	—
Rg_1, Rigor-1	3.6	—	—	—	—	195	—	—	—	7.3	93	68	—	—	—
Rg_2, Rigor-2	—	—	—	—	—	—	—	—	—	8	102	75	—	—	—
A, Activating	—	—	6	0.174	5.76	1.36	—	15	—	8	53	0.8	10	—	80
0S	—	0.019	5.98	—	—	—	0.81	15	—	8	68	15	10	—	80
5S	—	—	6	0.174	5.76	1.36	—	15	—	8	53	0.8	10	—	80
00D	—	—	6	0.058	2.79	0.076	—	15	—	8	62.6	9.2	10	—	80
0D	—	—	6	0.055	2.72	0.182	—	—	—	8	77.2	39.2	10	0.2	—
3D	—	—	6	0.205	2.86	—	2.786	—	11.9	8	42.0	21.4	10	0.2	—
WS	—	—	—	—	—	0.84	—	15	—	8	85.6	15	10	—	80
WD	—	—	—	—	2.78	0.10	—	—	—	8	95.4	39.2	10	0.2	—

CaEG, CaEGTA; CP, creatine phosphate; P = P_i = phosphate; Pr = Prop = proprionate; CK, creatine kinase. In addition, 10 mM morpholinopropane sulfonic acid is included in all of the solutions. The ionic strength of wash and activating solutions is 180 mM, and that of Sk, R, and Rg solutions is 200 mM. pCa of activating solutions is 4.40, Mg^{2+} concentration is 0.5 mM, and pH of all solutions is adjusted to 7.00 ± 0.01. 0S denotes the solution without ATP, 5S denotes the solution with 5 mM MgATP, 00D denotes the solution in which CP and CPK are included, 0D denotes the solution in which no CP/CPK or ADP is added, and 3D denotes the solution in which 3 mM $MgADP^-$ is present. See text for the WS and WD solutions.

processes (Kawai and Brandt, 1980). In brief, after being rinsed with WS solution (Table 1) in the MgATP study (WD in the MgADP study), a single skinned muscle fiber is maximally activated with an activating solution. When isometric tension reaches a steady state, the length of the fiber is changed in sine waves with varying frequencies (0.07–135 Hz, corresponding to 1.2–2300 ms), and the tension time course is collected. The amplitude of the length change is 0.125% L_0, which corresponds to 1.6 nm per half-sarcomere. The complex modulus $Y(f)$ is defined as the ratio of the stress change to the strain change in the frequency (f) domain and represented by a complex vector. The complex modulus contains both dynamic modulus and phase shift information. The dynamic modulus is defined as the length of the $Y(f)$ vector (= $|Y(f)|$), and the phase shift is defined as the angle from the abscissa of the $Y(f)$ vector (= arg[$Y(f)$]). The real part of the complex modulus is called the "elastic modulus" and the imaginary part the "viscous modulus." If the data are plotted as viscous modulus (ordinate) versus elastic modulus (abscissa) with the frequency as the intervening parameter, this plot is called the "Nyquist plot."

An examination of the Nyquist plot of slow twitch fibers (e.g. Fig. 3 C) reveals two hemicircles, thus we assume that Y(f) can be described by at least two exponenetial processes B, and C. In addition, process A is included at the low frequency end so that the results are consistent with those of rabbit psoas fibers. Since there is a mismatch between the data and the equation in the high frequency range, an additional exponential process D is introduced.

$$\begin{matrix} & \text{Process A} & \text{Process B} & \text{Process C} \\ Y(f) = H - A/(1 + a/\text{fi}) + B/(1 + b/\text{fi}) + C/(1 + c/\text{fi}) & & & \end{matrix} \quad (1)$$

$$\text{Process D}$$

$$+ D/(1 + d/\text{fi}),$$

where $i = \sqrt{-1}$. Lowercase letters a, b, c, and d ($a < b < c < d$) represent characteristic frequencies of exponential processes A, B, C, and D, respectively; uppercase letters A, B, C, and D represent their respective magnitudes. As in the case of ferret myocardium (Kawai et al., 1993), magnitude A is small in STFs. Characteristic frequencies multiplied by 2π are the apparent rate constants. H is the elastic modulus extrapolated to zero frequency; Y_∞ is the elastic modulus extrapolated to the infinite (∞) frequency and defined in Eq. 2:

$$Y_\infty = H + A - B + C + D \quad (2)$$

Y_∞ corresponds to phase 1 of the step analysis reported by Huxley and Simmons (1971). Y_∞ is also referred to as stiffness in this report. Process D corresponds to the fast component of phase 2, process C to the slow component of phase 2, process B to phase 3, and process A to phase 4 of step analysis.

RESULTS

Fast-twitch and slow-twitch fibers in rabbit soleus

Single fibers dissected from skinned rabbit soleus were activated in control activation solution A (Table 1). The phase shift is plotted against frequency in Fig. 1. We found that there are two different fiber types that demonstrated distinctive phase shift versus frequency plots. One type is shown in Fig. 1 by the solid line and filled circles. The other type is shown by the broken line and triangles. These two plots are similar in shape, but they are shifted along the abscissa by a factor of approximately 10. Each plot has a characteristic valley at low frequency and a characteristic peak at high frequency. Evidently, fibers that show the fast

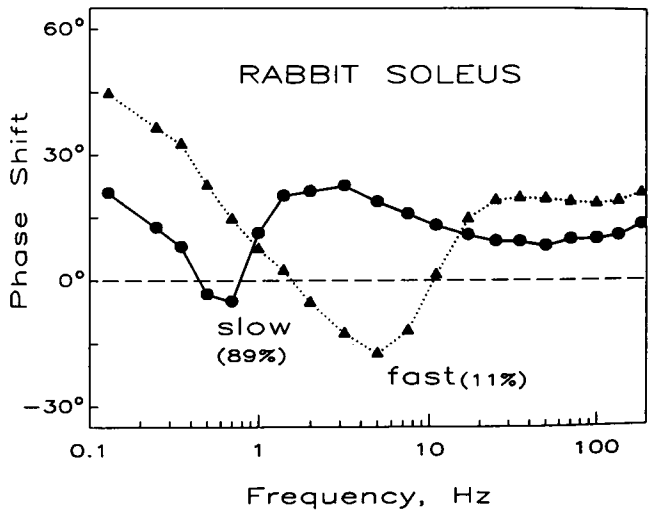

FIGURE 1 Sinusoidal length change was applied to single fibers from rabbit soleus muscle during maximum Ca^{2+} activation, the complex modulus data were obtained, and the phase shift is plotted against frequency ranging from 0.1 to 200 Hz on a lograthmic scale. The phase shift has the characteristic minimum and maximum. —●—, Slow-twitch fiber; ···▲···, fast-twitch fiber. We found that 89% of soleus is of the slow-twitch type, and 11% is of the fast-twitch type.

frequency response (triangles) are FTFs, and those that show the slow frequency response (circles) are STFs. We dissected a total of 215 single fibers from rabbit soleus and found that 192 fibers (89%) were of the slow-twitch type, and 23 fibers (11%) were of the fast-twitch type.

The complex modulus data were fitted to Eq. 1, and the characteristic frequencies a, b, c, and d were extracted. To examine the degree of separation between two fiber types, the number of fibers is plotted against characteristic frequencies b (Fig. 2 A) and c (Fig. 2 B) in the logarithmic scale. The data from rabbit psoas are also included in Fig. 2 for comparison. The separation of two fiber types in soleus is the greatest with characteristic frequency b (Fig. 2 A), and this is followed by characteristic frequency c (Fig. 2 B). We did not detect any overlap of frequencies between fast-twitch and slow-twitch fibers; thus identification of the fiber type was readily made based on the results of the sinusoidal analysis. Such a clear separation implies that the fibers we labeled soleus STFs are not the damaged soleus FTFs. Based on characteristic frequencies, we found that soleus FTFs (b = 6.3 ± 1.3 Hz, c = 22.3 ± 2.0, mean ± SD, N = 23) are faster than soleus STFs (b = 0.64 ± 0.11 Hz, c = 4.4 ± 1.4, N = 192), whereas soleus FTFs are slower than fast-twitch psoas fibers (b = 19.0 ± 1.4 Hz, c = 59.2 ± 4.8, N = 125). The results we report in this paper are data from fibers that are indicated by dark bars among soleus slow-twich fibers. These fibers had characteristic frequencies b and c of 0.56 ± 0.07 Hz and 3.6 ± 0.5 Hz, respectively (N = 15; eight fibers for MgATP study and seven fibers for MgADP study).

After seven or eight activations, the single STFs maintained a tension recovery higher than 80% (mean 90 ± 4% (SD), N = 15), the fibers maintained a sarcomere length of 2.5 μm, and

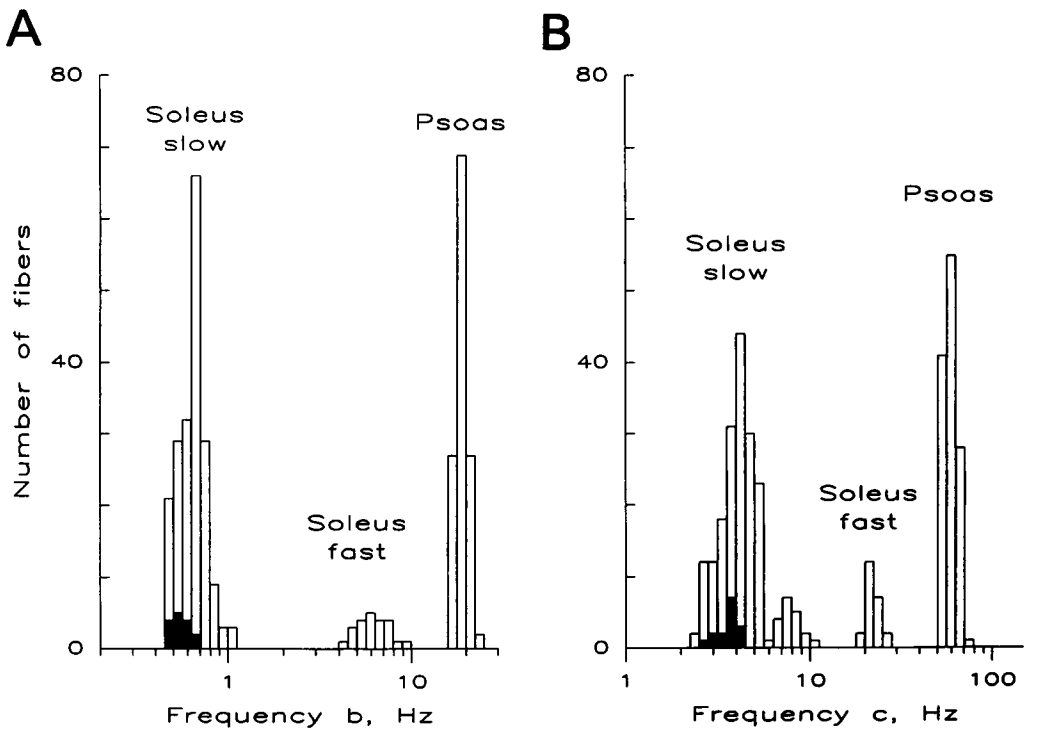

FIGURE 2 Distribution of the characteristic frequencies (Hz) of rabbit soleus STFs, soleus FTFs, and psoas fibers (white bars). The $\log_{10}$ of characteristic frequencies is first calculated, then one decade is divided into 20 equal sections in the lograthmic scale, and the histograms are constructed. Black bars represent soleus STFs that were used for ATP and ADP studies in the current report. (*A*) Distribution of the characteristic frequency *b*; the average *b* values of these groups are 0.64 ± 0.11 (n = 192), 6.3 ± 1.3 (n = 23), 19.0 ± 1.4 (n = 125), and 0.56 ± 0.07 (n = 15) for soleus STFs, soleus FTFs, psoas, and soleus STFs used for experiments, respectively. (*B*) Distribution of the characteristic frequency *c*; the average *c* values of respective groups are 4.4 ± 1.4 (n = 192), 22.3 ± 2.0 (n = 23), 59.2 ± 4.8 (n = 125), and 3.6 ± 0.5 (n = 15).

there was no abnormality detected in the entire length of the fibers under 200× Normarski optics (Leitz, Diavert).

Effects of MgATP on complex modulus

Single rabbit soleus STFs were activated with a series of MgATP solutions, and the complex modulus $Y(f)$ was collected at 20 different frequencies. The concentration of MgATP ranged from 0.05 to 5 mM. The results obtained from four MgATP concentrations are shown in the dynamic modulus versus frequency plot (Fig. 3 *A*), in the phase shift versus frequency plot (Fig. 3 *B*), and in the Nyquist plot (Fig. 3 *C*). As seen in Fig. 3 *A*, the dynamic modulus plot shifts to the right with an increase in the MgATP concentration. Similarly, the phase shift plot shifts to the right with an increase in the MgATP concentration (Fig. 3 *B*). These results indicate that cross-bridge kinetics become faster at higher MgATP concentrations. The general appearance of the Nyquist plots does not change with MgATP concentration (Fig. 3 *C*), indicating that no new processes are introduced or deleted with an increase in the MgATP concentration.

Effect of MgATP on the apparent rate constants

The complex modulus data were fitted to Eq. 1, and the apparent rate constants and their magnitude were extracted. The apparent rate constants $2\pi d$ and $2\pi c$ were averaged for eight experiments and plotted against the MgATP concentration in Fig. 4. As seen in these figures, both rate constants increased when the MgATP concentration was raised from 0.05 to 1 mM, and reached saturation when the MgATP concentration was raised further. The effect of MgATP on $2\pi d$ and $2\pi c$ is similar to our earlier reports on rabbit psoas (Kawai, 1978; Kawai and Halvorson, 1989; Zhao and Kawai, 1993) and ferret myocardium (Kawai et al., 1993). An examination of Fig. 4 *A* reveals that $2\pi d$ is a hyperbolic function of the MgATP concentration. Such a result is consistent with the following cross-bridge scheme:

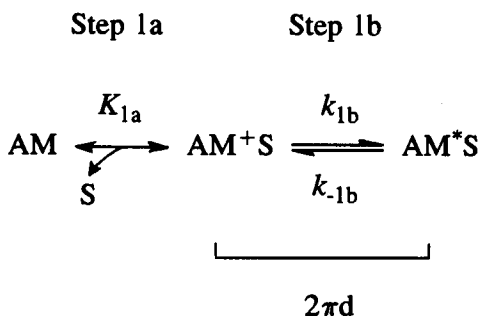

SCHEME 1

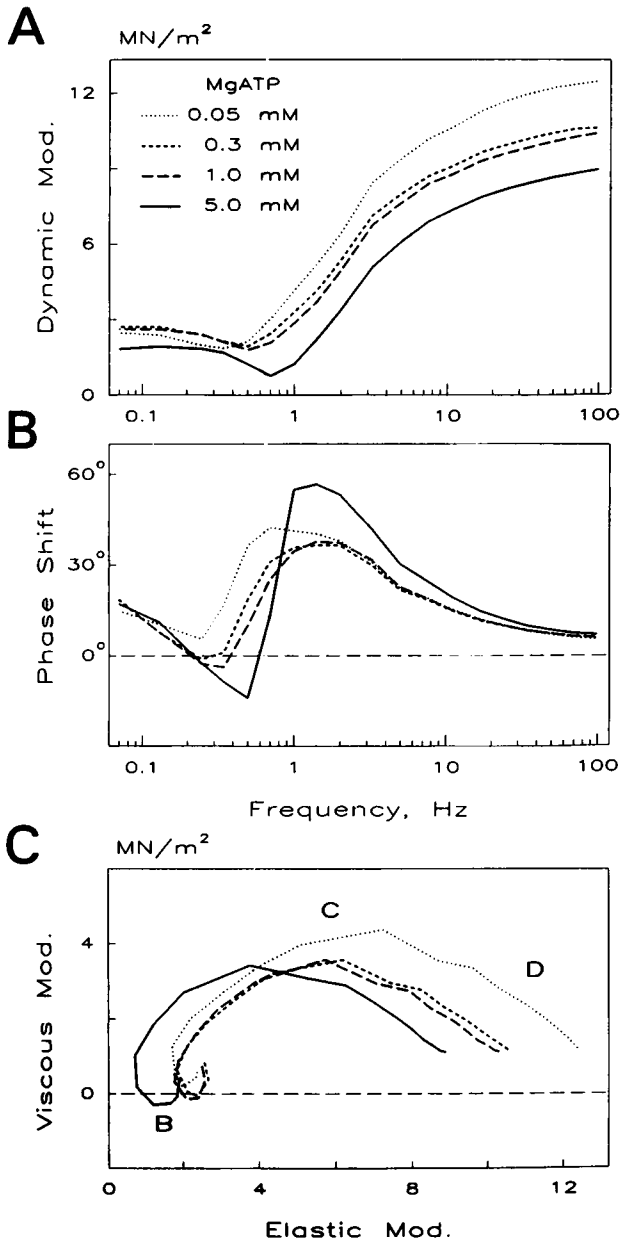

FIGURE 3 The effect of $MgATP^{2-}$ on the complex modulus $Y(f)$ of rabbit soleus is plotted in dynamic modulus [= $|Y(f)|$] versus frequency in *A*, in phase shift [= Arg $Y(f)$] versus frequency in *B*, and in viscous modulus [= Imag $Y(f)$] versus elastic modulus [= Real $Y(f)$] in *C* (Nyquist plot). The P_i concentration was fixed to 8 mM. The data represent the average of eight experiments. In the Nyquist plot (*C*), the low-frequency end is near the origin, and the high-frequency end is to the right of the plot. Three exponential processes B, C, and D are indicated in *C*. Process A is not indicated, because its magnitude is small and not well defined.

where A = actin, M = myosin, and S = MgATP. In step 1a, MgATP (S) binds to cross-bridges to form the collision complex AM^+S. In step 1b, AM^+S is isomerized to become AM*S. We assume that step 1b is monitored by process D. Equation 3 relates the rate and association constants of elementary steps to the apparent rate constant $2\pi d$ (Zhao and Kawai, 1993):

$$2\pi d = \frac{K_{1a}S}{1 + K_{1a}S}k_{1b} + k_{-1b}, \quad (3)$$

where S represents the MgATP concentration. Scheme 1 and Eq. 3 are the simplest ways of describing the data presented in Fig. 4 *A*, and no other scheme of the same degree of simplicity can describe the data.

Similarly, an examination of Fig. 4 *B* reveals that $2\pi c$ is a hyperbolic function of the MgATP concentration. This result is consistent with the following cross-bridge scheme:

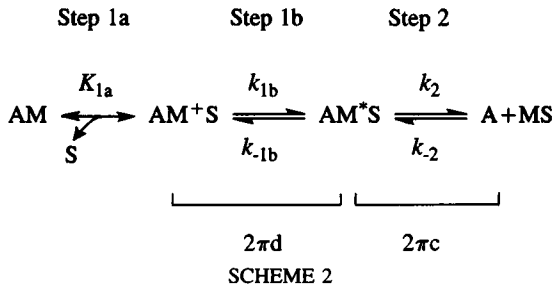

SCHEME 2

In this scheme step 2 is added to Scheme 1. Step 2 describes the cross-bridge detachment step, which is monitored by process C. Scheme 2 gives two apparent rate constants, $2\pi d$ and $2\pi c$. Of these, $2\pi d$ is the same as that given in Eq. 3, because $2\pi d \gg 2\pi c$ (Hammes, 1968; Zhao and Kawai, 1993). $2\pi c$ is given in Eq. 4 (Zhao and Kawai, 1993):

$$2\pi c = \frac{K_{1a}SK_{1b}}{1 + (1 + K_{1b})K_{1a}S}k_2 + k_{-2}, \quad (4)$$

where K_{1b} is the equilibrium constant of step 1b and is defined as $K_{1b} = k_{1b}/k_{-1b}$. Once again we emphasize that Scheme 2 and Eqs. 3 and 4 are the simplest ways of describing the data presented in Fig. 4 no other scheme of the same degree of simplicity can describe the data.

The data were fitted to Eqs. 3 and 4 simultaneously to deduce the rate constants and association constants of elementary steps. We found that $K_{1a} = 1.2 \pm 0.3\ mM^{-1}$ ($\pm$ SEM, $N = 8$). In Fig. 4, *A* and *B*, the curved lines represent theoretical projections based on Eqs. 3 and 4 and the best-fit parameters. The results are summarized in Table 2.

Effect of MgATP on isometric tension and stiffness (Y_∞)

Fig. 5 *A* demonstrates the relative tension of soleus STFs as a function of MgATP concentration. As seen in this figure, the isometric tension gradually decreased with an increase in the MgATP concentration. This decrease is consistent with earlier reports on skinned skeletal (Kawai, 1978; Ferenczi et al., 1984; Kawai and Halvorson, 1989; Pate et al.,

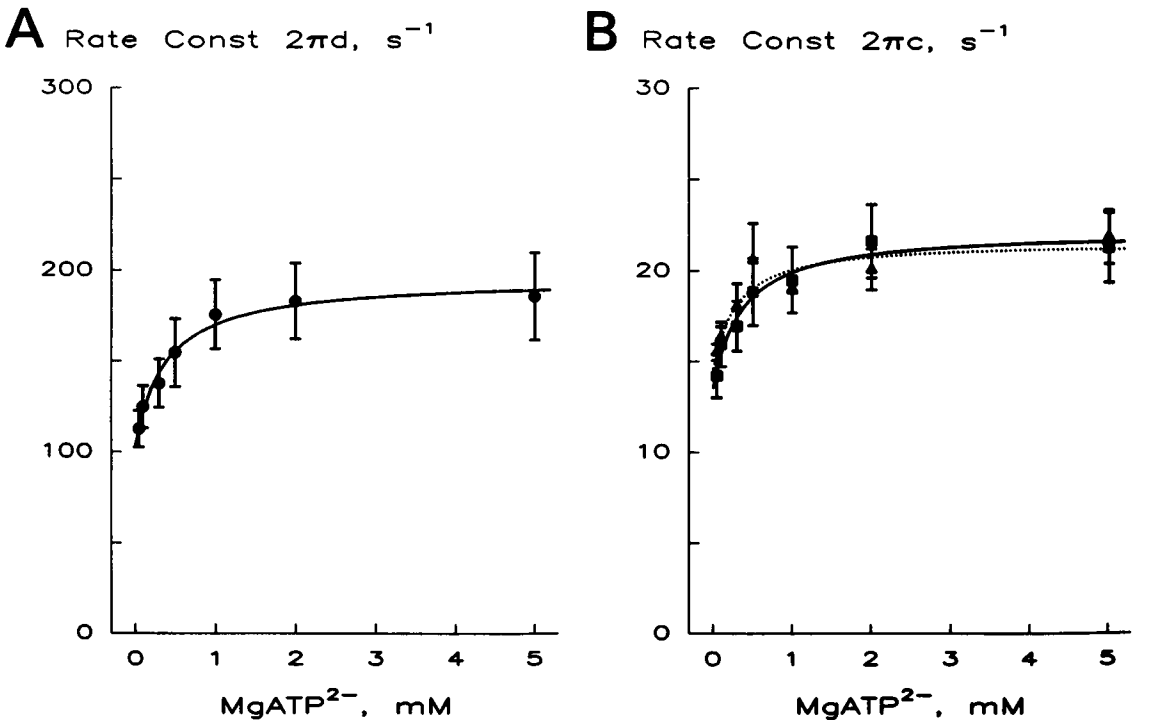

FIGURE 4 The apparent rate constants $2\pi d$ (in *A*) and $2\pi c$ (in *B*) are plotted against the $MgATP^{2-}$ concentration. The curved lines represent theoretical projections based on Eq. 3 and Eq. 4 with best-fit parameters. The data represent the average of eight experiments. (*B*) —■—, Data obtained at 80 units/ml CK; ···▲···, obtained at 160 units/ml CK.

1992), insect (Kuhn et al., 1985), and cardiac (Kawai et al., 1993) muscle preparations. Fig. 5 *B* represents stiffness (Y_∞) as a function of MgATP concentration. Similar to isometric tension, Y_∞ decreased as the MgATP concentration was raised, indicating that fewer cross-bridges were attached at higher MgATP concentration. In Fig. 5 *C* the tension-to-stiffness ratio is plotted against the MgATP concentration. This figure demonstrates that the ratio slightly increased as the MgATP concentration was elevated.

TABLE 2 The kinetic constants of elementary steps

Kinetic constant	Unit	Rabbit psoas* avg ± SEM (*n*)	Soleus STF avg ± SEM (*n*)	Soleus:psoas ratio
$K_0^{\#}$	mM^{-1}	2.27 ± 0.05 (7)	18 ± 4 (7)	7.8 ± 1.6
K_{1a}	mM^{-1}	0.52 ± 0.05 (7)	1.2 ± 0.3 (8)	2.2 ± 0.6
k_{1b}	s^{-1}	2600 ± 400 (7)	90 ± 20 (8)	0.036 ± 0.009
k_{-1b}	s^{-1}	1500 ± 100 (7)	100 ± 9 (8)	0.068 ± 0.008
K_{1b}	None	1.7 ± 0.2 (7)	1.0 ± 0.2 (8)	0.55 ± 0.15
k_2	s^{-1}	440 ± 30 (7)	21 ± 3 (8)	0.048 ± 0.008
k_{-2}	s^{-1}	147 ± 6 (7)	14.1 ± 1.0 (8)	0.096 ± 0.008
K_2	None	3.1 ± 0.3 (7)	1.6 ± 0.3 (8)	0.51 ± 0.05

*Results on rabbit psoas were based on data that used the same experimental solutions as in Table 1, except that ionic strength was adjusted to 200 mM and pCa was 4.66.

#K_0 was calculated based on $MgADP^-$ concentration, rather than the total MgADP concentration, as in our earlier reports (Kawai and Halvorson, 1989; Zhao and Kawai, 1993). The data from individual experiments were fitted to respective equations first, and then averaging was performed on the fitted parameters. The ratio is the result of the division of the averaged rabbit soleus value by the averaged rabbit psoas value.

Adequacy of the ATP regenerating system

It might be suspected that the creatine kinase (CK) concentration may not have been adequate in our experimental system to supply ATP and remove ADP. To rule out this possibility, we studied the effect of MgATP on the apparent rate constant $2\pi c$ at 160 units/ml CK and compared the result with that at 80 units/ml CK. As shown in Fig. 4 *B*, the effect of MgATP on $2\pi c$ is similar in these two cases. The ATP association constant (K_{1a}) deduced from the case of 160 units/ml CK is 0.92 ± 0.21 mM^{-1} (N = 4), not significantly different from that at 80 units/ml CK (1.2 ± 0.3 mM^{-1}, N = 8, Table 2). If the ATP-regenerating system were inadequate, K_{1a} would increase with an increase in the CK concentration. These results demonstrate that the CK concentration of 80 units/ml is adequate in rabbit soleus STFs under our experimental conditions. The concentration of creatine phosphate (CP) used in this study was 15 mM. We previously demonstrated that 15 mM CP was sufficient for supplying ATP and removing ADP in rabbit psoas fiber studies at 20°C (Zhao and Kawai, 1994a). Because the ATP hydrolysis rate is slower in soleus than in psoas, we conclude that 15 mM CP is sufficient in our studies using STFs.

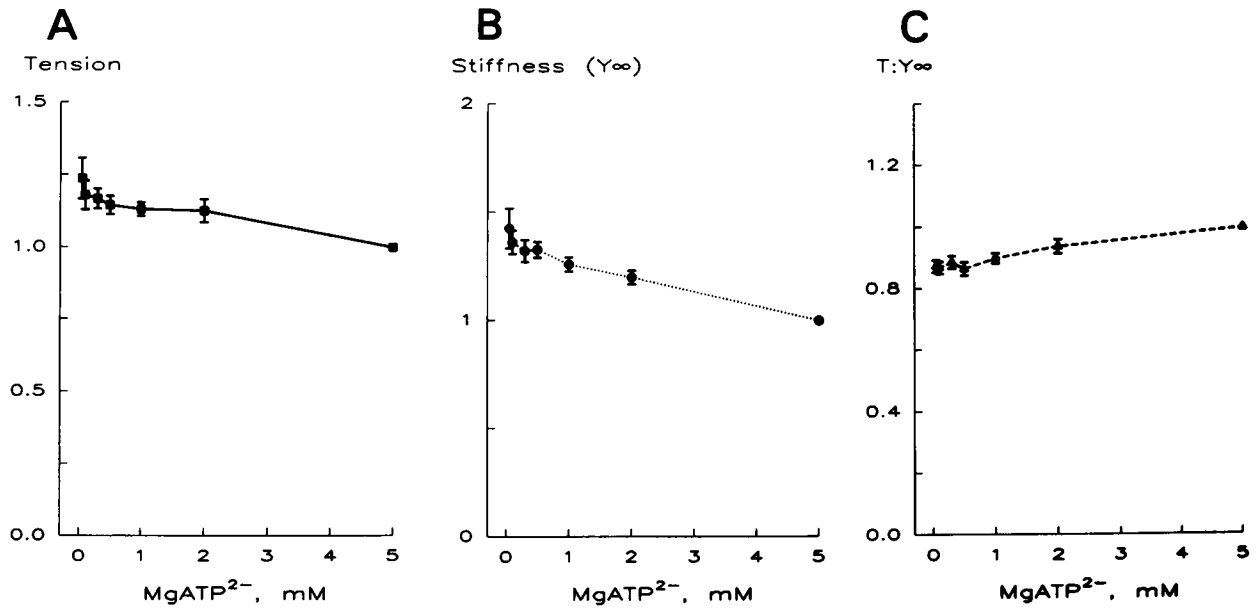

FIGURE 5 (*A*) Isometric tension is normalized to 5 mM $MgATP^{2-}$ and plotted against the $MgATP^{2-}$ concentration. The data represent the average of eight experiments. P_0 = 140 ± 20 kN/m^2 (N = 8, SEM). (*B*) Stiffness (Y_∞) of the same experiments is normalized to that at 5 mM $MgATP^{2-}$ and plotted against the $MgATP^{2-}$ concentration. Y_∞ = 8.8 ± 0.8 MN/m^2 (N = 8). (*C*) The ratio of tension to stiffness is plotted as a function of $MgATP^{2-}$ concentration. P_0/Y_∞ = 1.60 ± 0.13% L_0 (N = 8).

Effect of MgADP on the apparent rate constant $2\pi c$

To characterize the step involved in MgADP binding, the $MgADP^-$ concentration was changed (0–3 mM) at a fixed $MgATP^{2-}$ concentration (2 mM), and the apparent rate constants were obtained. In Fig. 6, $2\pi c$ is plotted against the $MgADP^-$ concentration. The $MgADP^-$ concentration, rather than the total ADP concentration, is plotted in the abcissa, because $MgADP^-$ is the molecular species that binds to cross-bridges. As seen in this figure, $2\pi c$ decreased hyperbolically with an increase in the $MgADP^-$ concentration. A similar ADP dependence was observed with $2\pi b$ and $2\pi d$ (data not shown). This observation is consistent with the reports on rabbit psoas fibers that MgADP decreases apparent rate constants (Kawai and Halvorson, 1989). Such ADP dependence can be explained in cross-bridge Scheme 3, in which step 0 is added to Scheme 2:

Equations that relate the rate constants of the elementary steps to the apparent rate constants are (Zhao and Kawai, 1993)

$$2\pi d = \frac{K_{1a}S}{1 + K_0D + K_{1a}S}k_{1b} + k_{-1b} \qquad (5)$$

$$2\pi c = \frac{K_{1a}SK_{1b}}{1 + K_0D + (1 + K_{1b})K_{1a}S}k_2 + k_{-2}, \qquad (6)$$

where D is the $MgADP^-$ concentration. As is evident, Eqs. 5 and 6 reduce to Eqs 3 and 4, respectively, as the $MgADP^-$ concentration approaches 0. The data of Fig. 6 were fitted to Eq. 6 using the values of K_{1a} and K_{1b} obtained from the MgATP study, and the theoretical projection is shown in Fig. 6 as a curved line. As seen in Fig. 6, the data fit well to Eq. 6, and K_0 was deduced to be 18 ± 4 mM^{-1} (N = 7).

In the ADP study, there is always a small amount of endogenous ADP present in the fiber, because of the continued ATP hydrolysis and the absence of the CP/CK system. This displaces the abcissa of Fig. 6 to the left. An additional solution (00D in Table 1), which contained CP and CK to inhibit the endogenous ADP production, but which was otherwise identical to 0D (the solution without added ADP, Table 1), was created to estimate the displacement (D_0). The complex modulus was collected in the 00D solution, $2\pi c$ was deduced, and the $2\pi c$ value was matched to that of the theoretical curve (Eq. 6). The D_0 value was obtained by extrapolation. We found D_0 to be 0.054 ± 0.016 mM (N = 7). Thus we conclude that there was an

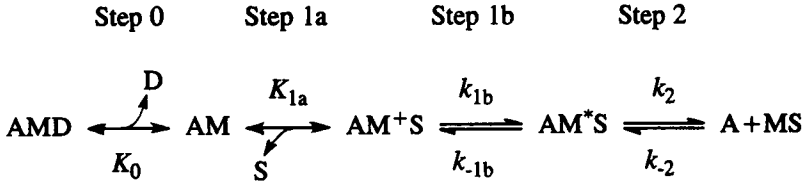

SCHEME 3

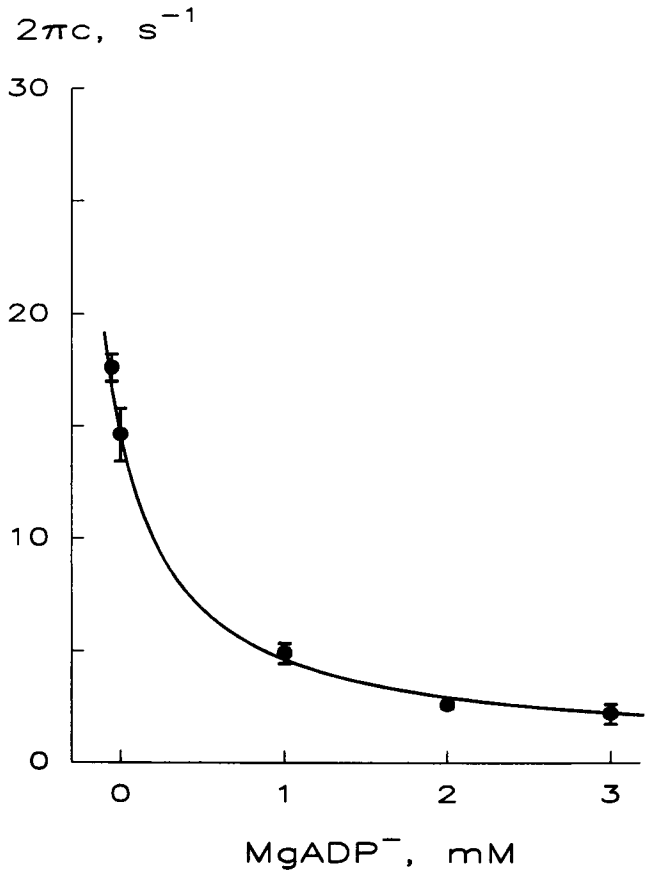

FIGURE 6 The effect of MgADP on the apparent rate constant $2\pi c$. The $MgATP^{2-}$ concentration was fixed to 2 mM, and the P_i concentration to 8 mM. The data represent the average of seven experiments. The curved line is a theoretical projection based on Eq. 5 and the best-fit parameters. D_0 was deduced to be 0.054 ± 0.016 mM.

average of 0.054 mM $MgADP^-$ present in the skinned rabbit soleus STFs when MgADP was not added to the activating solution and in the absence of CP or CPK. It is also possible to estimate D_0 by using the rate of ATP hydrolysis and the ADP diffusion constant (Cooke and Pate, 1985). Values of D_0 obtained from these methods are in agreement. Assuming that the ATPase rate of STFs is 3–8 times slower than that of psoas FTFs (Bárany, 1967; Reiser et al., 1985; Metzger and Moss, 1990; Potma et al., 1994), and D_0 has a value of 0.20 mM in fast-twitch psoas fibers (Cooke and Pate, 1985), our estimation of D_0 is about 0.025–0.067 mM.

Effect of MgADP on isometric tension and stiffness (Y_∞)

Isometric tension was normalized to that obtained from the control activating condition and plotted against the $MgADP^-$ concentration in Fig. 7 *A*. As seen in this figure, the tension increased as the $MgADP^-$ concentration was raised from 0 to 3 mM. This observation is consistent with the results obtained from rabbit psoas fibers (Cooke and Pate, 1985) and rabbit soleus fibers (Hoar et al., 1987). Fig. 7 *B* represents stiffness (Y_∞) as a function of $MgADP^-$ concentration. Y_∞ increased as the $MgADP^-$ concentration was raised, indicating that more cross-bridges were attached at a higher $MgADP^-$ concentration. In Fig. 7 *C* the tension-to-stiffness ratio is plotted against the $MgADP^-$ concentration. As seen in this figure, the ratio decreased slightly as the $MgADP^-$ concentration was raised.

DISCUSSION

Heterogenity of rabbit soleus muscle fibers

We found that there are two types of muscle fibers among rabbit soleus based on the phase shift versus frequency plot (Fig. 1). Our results indicate that the majority (89%) of rabbit soleus fibers are of the slow-twitch type, and the remainder (11%) are of the fast-twitch type. Their separation is unambiguously demonstrated based on sinusoidal analysis (Fig. 2). Such a clear separation implies that the fibers we labeled as soleus STFs are not the results of damaged soleus FTFs. The clear separation of STFs and FTFs by sinusoidal analysis, and their perfect correlation with light-chain isoforms as determined by sodium dodecyl sulfate-polyacrylamide gel electrophoresis was reported earlier (Kawai and Schachat, 1984). Similarly, Galler et al. (1994) reported a strong correlation between myosin heavy chain (MHC) isoform as detected by gradient sodium dodecyl sulfate-polyacrylamide gel electrophoresis and the time course of stretch activation in rat skeletal muscle fibers. The heterogenity of rabbit soleus fibers is not unexpected, as Staron and Pette (1987) reported that in rabbit soleus there are more than three types of fibers, the majority being type I slow-twitch fibers based on histochemical analysis. These type I fibers contain type I MHCs and slow-twitch-type myosin light chains (Kawai and Schachat, 1984; Reiser et al., 1985; Staron and Pette, 1987; Pette and Staron, 1990). Salviati et al. (1982) and Moore et al. (1987) reported that 1% of rabbit soleus fibers are of the fast-twitch type and 99% are of the slow-twitch type. Reiser et al. (1985) reported that 18% of the rabbit soleus fibers have higher V_{max} values than the remaining 82% fibers. Millar and Homsher (1992) reported that 2.5% of the soleus fibers are fast-twitch fibers. The difference in the relative abundance of FTFs in soleus may reflect the age and condition of the animals used for experiments. Alternatively, the difference may reflect the sampling procedure. It is possible that we have unintentionally isolated more FTFs than the population average, because our experience has shown that soleus FTFs are easier to dissect than soleus STFs.

Our results demonstrate that soleus FTFs are slower than fast-twitch psoas fibers (Fig. 2). It has been shown that psoas fibers consist of type IIb MHC, whereas soleus FTFs consist of type IIa MHC (Staron and Pette, 1987; Pette and Staron, 1990). The myosin light chains are predominantly of the fast type for soleus FTFs and psoas fibers (Staron and

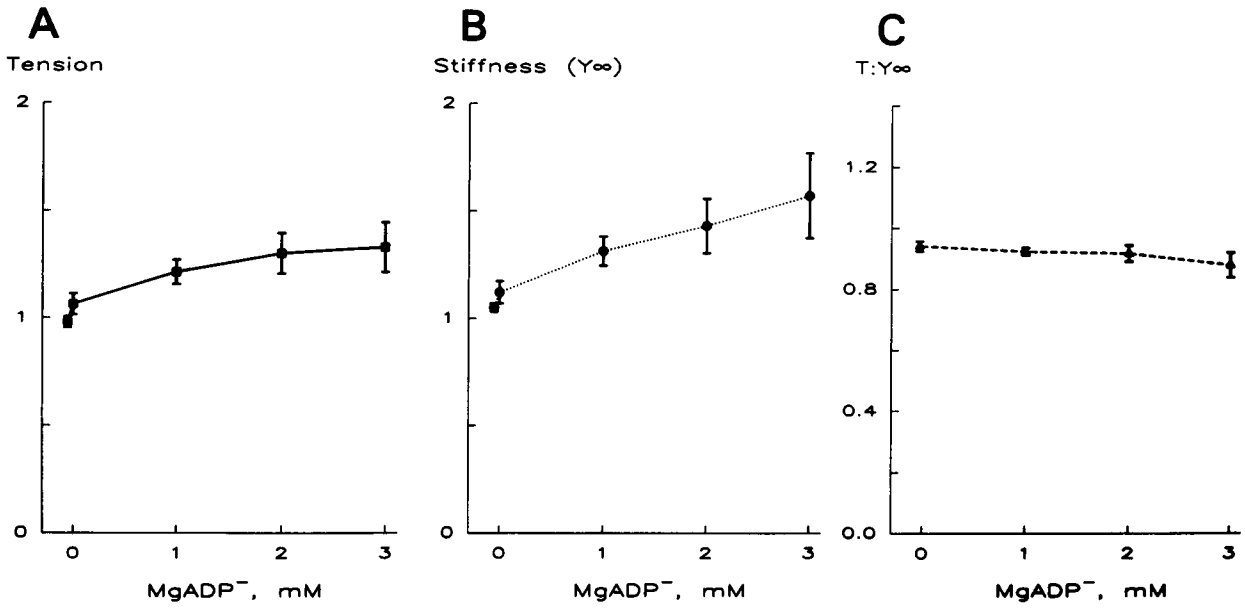

FIGURE 7 (*A*) Isometric tension was normalized to the individual values at control activation (5 mM $MgATP^{2-}$) and plotted as a function of $MgADP^-$ concentration ($N = 7$). The tension of the control activation was 150 ± 20 kN/m^2 ($N = 7$, SEM). (*B*) Stiffness (Y_∞) in the same experiments is normalized to that at control activation and plotted against the $MgADP^-$ concentration. Y_∞ of the control activation was 8.6 ± 0.7 MN/m^2 ($N = 7$, SEM). (*C*) The ratio of tension to stiffness (Y_∞) is plotted as a function of $MgADP^-$ concentration.

Pette, 1987; Pette and Staron, 1990). From these results, we infer that fibers with type IIa MHC are slower than those with type IIb MHC (Galler et al., 1994). In this report, single slow-twitch fibers rather than fast-twitch fibers from rabbit soleus were employed, and subsequent MgATP and MgADP studies were carried out to deduce the kinetic constants of elementary steps.

MgATP binding, isomerization, and cross-bridge detachment steps

To characterize the steps surrounding MgATP binding, we studied the effect of MgATP concentration on the apparent rate constants $2\pi c$ of exponential process C and $2\pi d$ of exponential process D. Processes C and D correlate to the slow component and fast component, respectively, of phase 2 in step analysis (Kawai and Zhao, 1993). As seen in Fig. 4, the two apparent rate constants increased when the MgATP concentration was raised to the low millimolar range, and this effect became saturated in the high millimolar range. The effect of MgATP on the rate constants $2\pi c$ and $2\pi d$ (Fig. 4) can be explained by cross-bridge Scheme 2. In this scheme we assumed that the ATP binding/dissociation reaction (step 1a) is very rapid, that process D maps to the isomerization step (step 1b), and that process C maps to the cross-bridge detachment step (step 2). These assumptions are consistent with the data, as indicated by the close fit of the data to the theoretical equations (Figs. 4 and 6). If the rate of ATP binding/dissociation reaction is comparable to the speed of the measurements, it follows that the $2\pi d$ or $2\pi c$ versus MgATP plot will become linear. This is apparently not the case, as shown in Fig. 4. If the mapping relation between process C and process D is reversed in Scheme 2, it follows that $2\pi d$ will become insensitive to the ATP concentration, because a slower reaction (process C) intervenes between ATP binding and process D. Apparently this is not the case either, as demonstrated in Fig. 4. Thus, we conclude that Scheme 2 uniquely describes the present data, and no other scheme can explain the data with the same degree of simplicity. The collision complex AM^+S and its isomerized form AM*S were recognized in earlier solution studies of extracted actin and myosin (Geeves et al., 1984).

From the MgATP study we deduced the kinetic constants of elementary steps K_{1a}, k_{1b}, k_{-1b}, k_2, and k_{-2} (Table 2). Table 2 also illustrates the kinetic constants obtained from rabbit psoas studied in the similar activating conditions for a comparative purpose. In STFs, K_{1a} is 1.2 mM^{-1}, which is 2.2 times the K_{1a} of rabbit psoas, indicating that MgATP binds to cross-bridges 2.2 times more strongly in soleus than in psoas. This observation is similar to our studies carried out on ferret myocardium, which reported that MgATP binds cross-bridges 4 times more strongly than psoas (Kawai et al., 1993). This observation is also consistent with the studies on the maximum shortening velocity (V_{max}). The K_m deduced from the plot of V_{max} versus MgATP concentration reciprocally correlates with K_{1a}. Stienen et al. (1988) reported that K_m is 3.5 times smaller in STFs than FTFs in *Xenopus laevis*. Pate et al. (1992) reported that K_m is 11 times smaller in soleus than in psoas. The conclusion that MgATP binds to cross-bridges more tightly in STFs than FTFs is consistent with the idea that in STFs, MgATP is

more effective in dissociating rigor cross-bridges (Pate et al., 1992).

We further found that the ATP isomerization and its reversal steps in soleus STF are 15 to 30 times slower than in psoas. However, there is not a large variation in the equilibrium constant K_{1b} among soleus STFs, psoas FTFs (Table 2), and ferret myocardium (Kawai et al., 1993). This latter result indicates that the free energy change associated with the ATP isomerization while bound to the cross-bridges is similar in these three different muscle types.

From the MgATP effect on the apparent rate constant $2\pi c$, we deduced the rate constants of the cross-bridge detachment step. k_2 and k_{-2} are 21 s^{-1} and 14 s^{-1}, respectively, and they compare with 440 s^{-1} and 147 s^{-1} for rabbit psoas, respectively (Table 2). Therefore, it can be concluded that in soleus STFs the cross-bridge detachment and its reversal steps are 10 to 20 times slower than in psoas. These results are at variance with the report that cross-bridge detachment is 3 times faster in soleus than psoas based on force-velocity measurement (Pate et al., 1992). The difference may be experimental or may be due to the method used to analyze the data. Force-velocity experiments are carried out while fibers are shortening isotonically, whereas the sinusoidal analysis experiments are carried out while fibers are held at near-isometric conditions. Our analysis of the data of Fig. 4 in terms of the cross-bridge Scheme 2 is a direct method that does not require many assumptions. The equilibrium constant of the cross-bridge detachment step K_2 differs by a factor of 2 between rabbit soleus STFs and rabbit psoas.

Stiffness (Y_∞) decreases as the MgATP concentration is increased (Fig. 5 *B*). This observation can be explained by noting that in Schemes 2 and 3 an addition of MgATP shifts the equilibrium to the right, so that more cross-bridges are in the detached state. Similarly, isometric tension decreases as the MgATP concentration is increased (Fig. 5 *A*), which can be explained in the same way. The tension-to-stiffness ratio increases slightly with an increase in the MgATP concentration (Fig. 5 *C*). This observation implies that cross-bridges at a low force state are shifted to a high force state as the MgATP concentration is elevated.

Inhibitory role of MgADP

As contrasted in Figs. 4 *B* and 6, MgADP has an effect that is the opposite of that of MgATP on the apparent rate constant $2\pi c$. This observation is consistent with reports on rabbit psoas fibers that demonstrated that MgADP decreases the apparent rate constants of exponential processes (Kawai and Halvorson, 1989), the maximum shortening velocity (V_{max}) (Cooke and Pate, 1985), and Ca^{2+}-activated ATPase activity (Sleep and Glyn, 1986). Similarly, it was reported that MgADP inhibits the Ca^{2+}-activated ATPase activity of actomyosin subfragment 1 isolated from rabbit psoas (Sleep and Glyn, 1986). It was also reported that MgADP inhibits Ca^{2+}-activated ATPase activity in rabbit soleus fibers (Hoar et al., 1987). Furthermore, as indicated in Figs. 5 and 7, MgADP has an effect that is the opposite of that of MgATP on the isometric tension, stiffness, and the tension-to-stiffness ratio. These antagonizing effects of MgADP and MgATP on muscle contraction are best explained in a model in which MgADP is a competitive inhibitor of MgATP and both nucleotides occupy the same binding site on the myosin head (Hill and Eisenberg, 1976; Cooke and Pate, 1985; Kawai and Halvorson, 1989; Dantzig et al., 1991). Scheme 3 incorporates the idea of the competitive inhibition of the effect of MgATP by MgADP.

Based on the effect of MgADP on the apparent rate constant $2\pi c$ (Fig. 6), the MgADP association constant K_0 was deduced. K_0 was found to be 8 times larger in STFs than in psoas (Table 2), indicating that MgADP binds to cross-bridges 8 times more tightly in soleus STFs than in psoas FTFs. This finding is reasonable, because as mentioned above, both MgADP and MgATP occupy the same nucleotide-binding site on the myosin head.

As shown in Fig. 7, *A* and *B*, isometric tension and stiffness increased as the $MgADP^-$ concentration was raised from 0 to 3 mM. This observation is due to the shift of population of different cross-bridge states, but not to the elevated Ca^{2+} sensitivity caused by $MgADP^-$ (Hoar et al., 1987). In Scheme 3, the addition of MgADP shifts the equilibrium to the left, thereby increasing the number of attached cross-bridges that are force-generating, and decreasing the number of detached cross-bridges. The tension-to-stiffness ratio decreases slightly with an elevation of $MgADP^-$ concentration (Fig. 7 *C*), indicating that cross-bridges shift from a high-force state to a low-force state as the $MgADP^-$ concentration is elevated.

Efficiency in energy utilization and muscle fatigue

In ^{31}P-NMR studies, it was demonstrated that slow-twitch muscles contain a smaller amount of ATP and CP than fast-twitch muscles (Meyer et al., 1985; Kushmerick, 1992a,b; McFarland et al., 1994). The short supply of ATP and CP may be compensated in part by the high binding affinity of MgATP to cross-bridges in slow-twitch muscles. The high affinity may be important when its supply becomes inadequate. For instance, when slow-twitch muscle fibers are fatigued, the ATP and CP concentrations decrease significantly, but the contractility of the fibers is not impaired proportionately in *Xenopus laevis* type 3 fibers (Nagesser et al., 1992) and rat soleus fibers (Fryer et al., 1995).

Comparison with cardiac muscle fibers

We found that the rate constants k_{1b}, k_{-1b}, and k_2 of rabbit soleus STFs (Table 2) are one-third to one-half of the respective rate constants in ferret myocardium (Kawai et al., 1993), whereas k_{-2} is about the same in both preparations. These observations are consistent with other studies. It was reported that rat soleus fibers have a k_{tr} value one-third of

that in rat cardiac muscles (Metzger and Moss, 1990; Wolff et al., 1995), and the rate of ATP hydrolysis may be slower in STFs than in cardiac muscles (Potma et al., 1994; Kentish and Stienen, 1994). We further found equilibrium constants K_{1a} and K_{1b} to be about the same in STF and cardiac preparations.

The Nyquist plots of rabbit soleus slow-twitch fibers in the control activating solution are similar to those from ferret myocardium. This observation is expected, because myosin heavy chains of soleus STF and the β-isoform of myosin heavy chain of myocardium are the same gene products (Sinha et al., 1984), and ferret myocardium consists primarily of β-isoform (MacKinnon et al., 1988).

We found that the $MgADP^-$ association constant of rabbit soleus STFs is about 8 times of that of psoas fibers. This result is similar to the difference between rabbit psoas and bovine myocardium studied in solutions and myofibrils. It was reported that the MgADP association constant of bovine myocardium is 16 to 29 times larger than that of rabbit psoas (White and Taylor, 1976; Greene and Eisenberg, 1980; Johnson and Adams, 1984; Siemankowski et al., 1985).

Possible artifacts in measurements

It may be suspected that end compliance influences our measurements. With our measurements, tension (P_0) during the control activation was 140 kN/m^2, stiffness (Y_∞) was 8.8 MN/m^2, and the tension:stiffness ratio (P_0/Y_∞) was 1.6% L_0. This ratio indicates the instantaneous length release required to abolish full tension. The ratio compares with 0.5% L_0 estimated from figure 4 of Brenner et al. (1982), measured at 5°C under the sarcomere length control in rabbit psoas fibers. This ratio is temperature sensitive (Zhao and Kawai, 1994b; S. Galler and K. Hilber, personal communication), and when adjusted to 20°C, the ratio becomes 0.7–0.9%. Assuming that this number is applicable to soleus STF, and if a 1.6% length release is imposed, then it follows that an extra 0.8% (= 1.6−0.8) would be imposed on compliant ends, and 0.8% on the central segment. These results imply that, in the case of sine waves, the amplitude of the length oscillation would have been 0.063% (= 0.125 × 0.8/1.6) instead of 0.125% in the central segment. Although this variation may underestimate elastic modulus extrapolated to infinity frequency (Y_∞), the variation may not affect rate constant measurements. This is because the complex modulus is the ratio of stress change to strain change, and the tension response is linear at this small length oscillation (Kawai and Brandt, 1980; Kawai et al., 1987). That is, if the strain change is half, the stress change would be half, giving rise to the same complex modulus. However, the above calculations should be considered with caution, because Brenner et al. (1982) did not correct for the mass of the tension transducer, which underestimates the tension:stiffness ratio. All of our data were corrected for the mass and viscosity of the tension transducer (see Appendix 1 of Kawai and Brandt, 1980). A direct analysis of the effect of end compliance was carried out by Shibata et al. (1987), who demonstrated that the characteristic minimum and maximum of the dynamic modulus versus frequency plot or the phase shift versus frequency plot are not affected, regardless of the use of the length of the central segment, end segment, or the total muscle length to measure the complex modulus in rabbit papillary muscles. Their results imply that characteristic frequencies a, b, c, and d are not affected whether the central segment length is controlled or not. Thus the existence of compliant ends may not affect the measured rate constants. Alternatively, the compliance at the ends may be totally passive, and the measured rate constants would be a fixed fraction of the cross-bridge rate constants (Luo et al., 1993). This fraction remains approximately the same when cross-bridges are maximally activated in saturating Ca^{2+}. Therefore, qualitative features of the effects of MgATP and MgADP are not changed when the presence of the compliant ends is considered. From these considerations we conclude that the equilibrium constants are not affected, even if the compliant ends are considered.

CONCLUSIONS

We demonstrate that cross-bridge Scheme 3 uniquely describes the effects of MgATP and MgADP on the apparent rate constants and tension of rabbit soleus slow-twitch fibers. No other scheme can describe the data with the same degree of simplicity. In STFs, MgATP binds to cross-bridges 2.2 times more tightly than rabbit psoas, indicating that cross-bridges of STFs are more resistant to ATP depletion than are FTFs. Similarly, MgADP binds to cross-bridges of STFs 8 times more tightly than to those of rabbit psoas. We further demonstrate that the rate constants of ATP isomerization (k_{1b}, k_{-1b}) and cross-bridge detachment (k_2, k_{-2}) are generally an order of magnitude slower than that of rabbit psoas.

We thank Miss Karen Humphries for carrying out the comparative experiments on rabbit psoas fibers. This study was supported by grants from NSF IBN 93-18120 and AHA (Iowa affiliate) IA-94-GS-45.

REFERENCES

Bárany, M. 1967. ATPase activity of myosin correlated with speed of muscle shortening. *J. Gen. Physiol.* 50(Suppl P2):197–218.

Brenner, B., M. Schoenberg, J. M. Chalovich, L. E. Greene, and E. Eissenberg. 1982. Evidence for cross-bridge attachment in relaxed muscle at low ionic strength. *Proc. Natl. Acad. Sci. USA.* 79:7288–7291.

Cooke, R., and E. Pate. 1985. The effects of ADP and phosphate on the contraction of muscle fibers. *Biophys. J.* 48:789–798.

Crow, M. T., and M. J. Kushmerick. 1982. Chemical energetics of slow- and fast-twitch muscles of the mouse. *J. Gen. Physiol.* 79:147–166.

Dantzig, J. A., M. G. Hibberd, D. R. Trentham, and Y. E. Goldman. 1991. Cross-bridge kinetics in the presence of MgADP investigated by photolysis of caged ATP in rabbit psoas muscle fibres. *J. Physiol. (Lond.).* 432:639–680.

Ferenczi, M. A., Y. E. Goldman, and R. M. Simmons. 1984. The dependence of force and shortening velocity on substrate concentration in skinned muscle fibers from *Rana temporaria*. *J. Physiol. (Lond.).* 350:519–543.

Fryer, M. W., V. J. Owen, G. D. Lamb, and D. G. Stephenson. 1995. Effects of creatine phosphate and P_i on Ca^{2+} movements and tension development in rat skinned skeletal muscle fibers. *J. Physiol. (Lond.).* 482:123–140.

Galler, S., T. L. Schmitt, and D. Pette. 1994. Stretch activation, unloaded shortening velocity, and myosin heavy chain isoforms of rat skeletal muscle fibers. *J. Physiol. (Lond.).* 478:513–521.

Geeves, M. A., R. S. Goody, and H. Gutfreund. 1984. Kinetics of acto-S1 interaction as a guide to a model for the cross-bridge cycle. *J. Muscle Res. Cell Motil.* 5:351–361.

Godt, R. E., and D. W. Maughan. 1988. On the composition of the cytosol of relaxed skeletal muscle of the frog. *Am. J. Physiol.* 254:C591–C604.

Greene, L. E., and E. Eisenberg. 1980. Dissociation of the actin-subfragment 1 complex by adenyl-5′-yl imidodiphosphate, ADP, and PP_i. *J. Biol. Chem.* 255:543–548.

Hammes, G. G. 1968. Relaxation spectrometry of biological systems. *Adv. Protein Chem.* 23:1–57.

Hoar, P. E., C. W. Mahoney, and W. G. L. Kerrick. 1987. MgADP increases maximum tension and Ca^{2+} sensitivity in skinned rabbit soleus fibers. *Pflugers Arch.* 410:30–36.

Huxley, A. F., and R. M. Simmons. 1971. Proposed mechanism of force generation in striated muscle. *Nature.* 233:533–538.

Johnson, R. E., and P. Adams. 1984. ADP binds similarly to rigor muscle myofibrils and to actomyosin subfragment one. *FEBS Lett.* 174:11–14.

Kawai, M. 1978. Head rotation or dissociation? A study of exponential rate processes in chemically skinned rabbit muscle fibers when MgATP concentration is changed. *Biophys. J.* 22:97–103.

Kawai, M., and P. W. Brandt. 1980. Sinusoidal analysis: a high resolution method for correlating biochemical reactions with physiological processes in activated skeletal muscles of rabbit, frog and crayfish. *J. Muscle Res. Cell Motil.* 1:279–303.

Kawai, M., and H. R. Halvorson. 1989. Role of MgATP and MgADP in the crossbridge kinetics in chemically skinned rabbit psoas fibers. Study of a fast exponential process (C). *Biophys. J.* 55:595–603.

Kawai, M., and H. R. Halvorson. 1991. Two step mechanism of phosphate release and the mechanism of force generation in chemically skinned fibers of rabbit psoas muscle. *Biophys. J.* 59:329–342.

Kawai, M., Y. Saeki, and Y. Zhao. 1993. Cross-bridge scheme and kinetic constants of elementary steps deduced from chemically skinned papillary and trabecular muscles of the ferret. *Circ. Res.* 73:35–50.

Kawai, M., and F. H. Schachat. 1984. Differences in the transient response of fast and slow skeletal muscle fibers: correlations between complex modulus and myosin light chain. *Biophys. J.* 45:1145–1151.

Kawai, M., and Y. Zhao. 1993. Cross-bridge scheme and force per cross-bridge state in skinned rabbit psoas muscle fibers. *Biophys. J.* 65:638–651.

Kentish, J. C., and G. J. Stienen. 1994. Differential effects of length on maximum force production and myofibrillar ATPase activity in rat skinned cardiac muscle. *J. Physiol. (Lond.).* 475:175–184.

Kuhn, H. J., C. Bletz, K. Güth, and J. C. Rüegg. 1985. The effect of MgATP on forming and breaking actin-myosin linkages in contracted skinned insect flight muscle fibres. *J. Muscle Res. Cell Motil.* 6:5–27.

Kushmerick, M. J., R. A. Meyer, and T. R. Brown. 1992a. Regulation of oxygen consumption in fast- and slow-twitch muscle. *Am. J. Physiol.* 263:C598–C606.

Kushmerick, M. J., T. S. Moerland, and R. W. Wiseman. 1992b. Mammalian skeletal muscle fibers distiguished by contents of phosphocreatine, ATP, and P_i. *Proc. Natl. Acad. Sci. USA.* 89:7521–7525.

Luo, Y., R. Cooke, and E. Pate. 1993. A model of stress relaxation in cross-bridge systems: effect of a series elastic element. *Am. J. Physiol.* 265:C279–C288.

MacKinnon, R., J. K. Gwathmey, P. D. Allen, G. M. Briggs, and J. P. Morgan. 1988. Modulation by the thyroid state of intracellular calcium and contractility in ferret ventricular muscle. *Circ. Res.* 63:1080–1089.

Marston, S. B., and E. W. Taylor. 1980. Comparison of the myosin and actomyosin ATPase mechanisms of the four types of vertebrates muscles. *J. Mol. Biol.* 139:573–600.

McFarland, E. W., M. J. Kushmerick, and T. S. Moerland. 1994. Activity of creatine kinase in a contracting mammalian muscle of uniform fiber type. *Biophys. J.* 67:1912–1924.

Metzger, J. M., and R. L. Moss. 1990. Calcium-sensitive cross-bridge transitions in mammalian fast and slow skeletal muscle fibers. *Science.* 247:1088–1090.

Meyer, R. A., T. R. Brown, and M. J. Kushmerick. 1985. Phosphorus nuclear magnetic resonance of fast- and slow-twitch muscle. *Am. J. Physiol.* 248:C279–C287.

Millar, N. C., and E. Homsher. 1992. Kinetics of force generation and phosphate release in skinned rabbit soleus muscle fibers. *Am. J. Physiol.* 252:C1239–C1245.

Moore, G. E., M. M. Briggs, and F. H. Schachat. 1987. Patterns of troponin T expression in mammalian fast, slow and promiscuous muscle fibers. *J. Muscle Res. Cell Motil.* 8:13–22.

Nagesser, A. S., W. J. van der Lararse, and G. Elzinga. 1992. Metabolic changes with fatigue in different types of single muscle fibers of *Xenopus laevis*. *J. Physiol. (Lond.).* 448:511–523.

Pate, E., M. Lin, K. Franks-Skiba, and R. Cooke. 1992. Contraction of glycerinated rabbit slow-twitch muscle fibers as a function of MgATP concentration. *Am. J. Physiol.* 262:C1039–C1046.

Pette, D., and R. S. Staron. 1990. Cellular and molecular diversities of mammalian skeletal muscle fibers. *Rev. Physiol. Biochem. Pharmacol.* 116:2–47.

Potma, E. J., I. A. van Graas, and G. J. M. Stienen. 1994. Effects of pH on myofibrillar ATPase activity in fast and slow skeletal muscle fibers of the rabbit. *Biophys. J.* 67:2404–2410.

Reiser, P. J., R. L. Moss, G. G. Giulian, and M. L. Greaser. 1985. Shortening velocity in single fibers from adult rabbit soleus muscles is correlated with myosin heavy chain composition. *J. Biol. Chem.* 260: 9077–9080.

Salviati, G., R. Betto, and D. Daniell-Betto. 1982. Polymorphism of myofibrillar proteins of rabbit skeletal-muscle fibers. *Biochem. J.* 207:261–272.

Shibata, T., W. C, Hunter, A. Yang, and K. Sagawa. 1987. Dynamic stiffness measured in central segment of excised rabbit papillary muscles during barium contracture. *Circ. Res.* 60:756–769.

Siemankowski, R. F., M. O. Wiseman, and H. D. White. 1985. ADP dissociation from actomyosin subfragment 1 is sufficiently slow to limit the unloaded shortening velocity in vertebrate muscle. *Proc. Natl. Acad. Sci. USA.* 82:658–662.

Sinha, A. M., D. J. Friedman, J. M. Nigro, S. Jakovcic, M. Rabinowitz, and P. K. Umeda. 1984. Expression of rabbit ventricular α-myosin heavy chain messanger RNA sequences in atrial muscle. *J. Biol. Chem.* 259: 6674–6680.

Sleep, J., and H. Glyn. 1986. Inhibition of myofibrillar and actomyosin subfragment 1 adenosinetriphosphatase by adenosine 5′-diphosphate, pyrophosphate, and adenyl-5′-yl imdodiphosphate. *Biochemistry.* 25: 1149–1154.

Staron, R. S., and D. Pette. 1987. The multiplicity of combinations of myosin light chains and heavy chains in histochemically typed single fibers (rabbit soleus muscle). *Biochem. J.* 243:687–693.

Stienen, G. J. M., W. J. van der Laarse, and G. Elzinga. 1988. Dependence of the force-velocity relationship on MgATP in different types of muscle fibers from *Xenopus laevis*. *Biophys. J.* 53:849–855.

Wang, G., and M. Kawai. 1995. Temperature effect on elementary steps of the cross-bridge cycle in rabbit soleus muscle fibers. *Biophys. J.* 68:A17. (Abstr.)

Wang, G., Y. Zhao, and M. Kawai. 1994. Elementary steps of the cross-bridge cycle in rabbit soleus muscle fibers. *Biophys. J.* 66:A304. (Abstr.)

White, H. D., and E. W. Taylor. 1976. Energetics and mechanism of actomyosin adenosin triphosphate. *Biochemistry.* 15:5818–5826.

Wolff, M. R., K. S. McDonald, and R. L. Moss. 1995. Rate of tension development in cardiac muscle varies with level of activator calcium. *Circ. Res.* 76:154–160.

Zhao, Y., and M. Kawai. 1993. The effect of the lattice spacing on cross-bridge kinetics in chemically skinned psoas fibers. II. Elementary steps affected by the spacing change. *Biophys. J.* 64:197–210.

Zhao, Y., and M. Kawai. 1994a. BDM affects nucleotide binding and force generation steps of the cross-bridge cycle in rabbit psoas muscle fibers. *Am. J. Physiol.* 266:C437–C447.

Zhao, Y., and M. Kawai. 1994b. The kinetic and thermodynamic studies of the cross-bridge cycle in rabbit psoas muscle fibers. *Biophys. J.* 67:1655–1668.